# Measurement of the Isolated Nuclear Two-Photon Decay in $^{72}$Ge

D. Freire-Fernández,[1,2,†] W. Korten,[3,‡] R. J. Chen,[4,5] S. Litvinov,[4] Yu. A. Litvinov,[4] M. S. Sanjari,[4,6] H. Weick,[4] F. C. Akinci,[7] H. M. Albers,[4] M. Armstrong,[4,8] A. Banerjee,[4] K. Blaum,[1] C. Brandau,[4] B. A. Brown,[9] C. G. Bruno,[10] J. J. Carroll,[11] X. Chen,[12] C. J. Chiara,[11] M. L. Cortes,[13] S. F. Dellmann,[14] I. Dillmann,[15,16] D. Dmytriiev,[4] O. Forstner,[4,17,18] H. Geissel,[4,*] J. Glorius,[4] A. Görgen,[19] M. Górska,[4] C. J. Griffin,[15] A. Gumberidze,[4] S. Harayama,[20] R. Hess,[4] N. Hubbard,[4,13] K. E. Ide,[13] Ph. R. John,[13] R. Joseph,[4] B. Jurado,[21] D. Kalaydjieva,[3] Kanika,[2,4] F. G. Kondev,[22] P. Koseoglou,[13] G. Kosir,[28] Ch. Kozhuharov,[4] I. Kulikov,[2,4] G. Leckenby,[15,23] B. Lorenz,[4] J. Marsh,[10] A. Mistry,[4,13] A. Ozawa,[24] N. Pietralla,[13] Zs. Podolyák,[25] M. Polettini,[26,27] M. Sguazzin,[21] R. S. Sidhu,[1,4,10] M. Steck,[4] Th. Stöhlker,[4,17,18] J. A. Swartz,[21] J. Vesic,[28] P. M. Walker,[25] T. Yamaguchi,[20,29] and R. Zidarova[13]

[1]*Max-Planck-Institut für Kernphysik, 69117 Heidelberg, Germany*
[2]*Ruprecht-Karls-Universität Heidelberg, 69120 Heidelberg, Germany*
[3]*IRFU, CEA, Université Paris-Saclay, Gif-sur-Yvette, 91191, France*
[4]*GSI Helmholtzzentrum für Schwerionenforschung GmbH, 64291 Darmstadt, Germany*
[5]*CAS Key Laboratory of High Precision Nuclear Spectroscopy and Center for Nuclear Matter Science, Institute of Modern Physics, Chinese Academy of Sciences, Lanzhou 730000, People's Republic of China*
[6]*Aachen University of Applied Sciences, Aachen, Germany*
[7]*Department of Physics, Istanbul University, 34134 Istanbul, Turkey*
[8]*Institut für Kernphysik, Universität zu Köln, 50937 Cologne, Germany*
[9]*Department of Physics and Astronomy, and the Facility for Rare Isotope Beams, Michigan State University, East Lansing, Michigan 48824-1321, USA*
[10]*School of Physics and Astronomy, University of Edinburgh, Edinburgh EH9 3JZ, United Kingdom*
[11]*U.S. Army Combat Capabilities Development Command Army Research Laboratory, Adelphi, Maryland 20783, USA*
[12]*Faculty of Science and Engineering, University of Groningen, 9701 BA Groningen, The Netherlands*
[13]*Technische Universität Darmstadt, Department of Physics, Institute for Nuclear Physics, 64289 Darmstadt, Germany*
[14]*Goethe-Universität, 60438 Frankfurt, Germany*
[15]*TRIUMF, Vancouver, BC V6T 2A3, Canada*
[16]*Department of Physics and Astronomy, University of Victoria, Victoria, BC V8P 5C2, Canada*
[17]*Institute of Optics and Quantum Electronics, Friedrich Schiller University Jena, 07743 Jena, Germany*
[18]*Helmholtz Institute Jena, 07743 Jena, Germany*
[19]*Department of Physics, University of Oslo, 0316 Oslo, Norway*
[20]*Department of Physics, Saitama University, Saitama, 338-8570, Japan*
[21]*Université de Bordeaux, CNRS, LP2I Bordeaux, 33170 Gradignan, France*
[22]*Physics Division, Argonne National Laboratory, Lemont, Illinois 60439, USA*
[23]*Department of Physics and Astronomy, The University of British Columbia, Vancouver, British Columbia V6T 1Z1, Canada*
[24]*Institute of Physics, University of Tsukuba, Tsukuba, 305-8571, Ibaraki, Japan*
[25]*School of Mathematics and Physics, University of Surrey, Guildford, GU2 7XH, United Kingdom*
[26]*Dipartimento di Fisica, Università degli Studi di Milano, 20133, Milan, Italy*
[27]*Istituto Nazionale di Fisica Nucleare, Sezione di Milano, 20133, Milan, Italy*
[28]*Jožef Stefan Institute, Ljubljana 1000, Slovenia*
[29]*Tomonaga Center for the History of the Universe, University of Tsukuba, Tsukuba, 305-8571, Ibaraki, Japan*

(Received 18 December 2023; revised 16 March 2024; accepted 14 May 2024; published 11 July 2024)

The nuclear two-photon or double-gamma ($2\gamma$) decay is a second-order electromagnetic process whereby a nucleus in an excited state emits two gamma rays simultaneously. To be able to directly measure the $2\gamma$ decay rate in the low-energy regime below the electron-positron pair-creation threshold, we combined the isochronous mode of a storage ring with Schottky resonant cavities. The newly developed technique can be applied to isomers with excitation energies down to ~100 keV and half-lives as short as

~10 ms. The half-life for the $2\gamma$ decay of the first-excited $0^+$ state in bare $^{72}$Ge ions was determined to be 23.9(6) ms, which strongly deviates from expectations.

DOI: 10.1103/PhysRevLett.133.022502

The nuclear two-photon decay or double-gamma ($2\gamma$) involves the decay of an excited nucleus through the simultaneous emission of two $\gamma$ rays via the virtual excitation of intermediate states, $I_n$. The partial half-life of this decay gives access to observables such as the (transitional) electromagnetic polarizability and susceptibility, which are important ingredients in constraining parameters of the nuclear equation of state [1], determining the neutron skin thickness [2], and constraining the nuclear matrix elements of the neutrinoless double-beta decay [3].

This second-order quantum-mechanical process, initially formulated for the case of atomic transitions by Göppert-Mayer [4,5], was later extended to nuclear transitions. The early theoretical description utilizing second-order perturbation theory [6,7] was completed by Friar *et al.* [8,9] and later generalized by considering not only dipole but also higher multipolarities by Kramp *et al.* [10], who derived the total $2\gamma$ decay probability for $0^+ \rightarrow 0^+$ ($E0$) transitions [see Eq. (A.42) in [10] ]:

$$W_{\gamma\gamma} = \frac{\omega_0^7}{105\pi}\left[\alpha_{E1}^2 + \chi_{M1}^2 + \omega_0^4 \frac{\alpha_{E2}^2}{4752}\right] = \frac{\omega_0^7}{105\pi} M_{\gamma\gamma}^2, \qquad (1)$$

where $\omega_0$ denotes the energy difference between the initial and final state, while $\alpha$ and $\chi$ denote the electric transition polarizability and the magnetic transition susceptibility, respectively. The sum of terms within the brackets is equivalent to the squared magnitude of the cumulative nuclear matrix element, denoted as $M_{\gamma\gamma}^2$. These observables describe the difference of the electric polarizabilities and magnetic susceptibilties between the two $0^+$ states and are complementary to the standard nuclear polarizabilities and susceptibilities, which describe the response of the nucleus to a perturbation by electromagnetic fields, and are related to changes of the nuclear charge distribution and currents inside the nucleus.

All previous experiments conducted to date have employed $\gamma$-ray spectroscopy in order to investigate the two-photon decay, as demonstrated in the studies referenced in [11–15]. However, the main challenge lies in distinguishing the relatively small signal of the two simultaneously emitted photons from other (direct or indirect) photon sources, such as single-photon decay, internal pair creation (IPC), or internal-conversion (IC) electrons, due to the continuous energy spectrum associated with the two-photon emission. Therefore, ideally, the search for nuclear $2\gamma$ decays is conducted in even-even (e–e) nuclei with a first excited $0^+$ state, since the emission of a single $\gamma$ ray is forbidden. In fact, the only cases where the $2\gamma$ decay of a $0^+ \rightarrow 0^+$ transition was successfully observed using $\gamma$-ray spectroscopy are $^{16}$O, $^{40}$Ca, and $^{90}$Zr [10,16]. In these cases, the excited $0^+$ states are located at high excitation energies and the observed branching ratios for the $2\gamma$ decay are of the order of $10^{-4}$. The most surprising result is that the contribution from two subsequent $M1$ ($2M1$) transitions and $2E1$ transitions are of a similar strength, while naively a dominance of the $2E1$ decay would be expected. This has been explained by a strong cancellation effect in the electric-dipole transition polarizability in these doubly magic nuclei. This cancellation effect is related to the different structure of the two $0^+$ states, i.e., different contributions from $0p-0h$ and $np-nh$ excitations across the closed shells [17].

Excited $0^+$ states at low energy are a very important evidence for nuclear shape coexistence [18], however, their identification is challenging since it usually requires observation of conversion electrons. This is experimentally much more difficult than detecting $\gamma$ rays due to the strong background from atomic electrons, abundantly produced in nuclear reactions, or from $\beta$ decay. Such states are only known in a handful of nuclei across the whole nuclear chart [19], among which only $^{72}$Ge and $^{98}$Mo are stable. Low-lying $0^+$ states, i.e., at energies below the IPC threshold (1.022 MeV), have been found in unstable nuclei, often located far from the valley of stability, and thus requiring the use of radioactive ion beams. One of the most notable cases is $^{186}$Pb, where two excited $0^+$ states below 1 MeV have been discovered and interpreted as evidence for a unique triple shape coexistence [20]. Another notable example is the $N=Z$ nucleus $^{72}$Kr where the existence of an excited $0^+$ state has been speculated for several decades, before it was finally seen in conversion-electron spectroscopy [21]. In view of the experimental difficulties, it is possible, or maybe even likely, that many more unstable nuclei with a low-lying first excited $0^+$ state exist, but have so far escaped observation. Besides their importance for a better understanding of the nuclear structure, $0^+$ isomers in $N \approx Z$ nuclei, like $^{72}$Kr, may also play a vital role in the nucleosynthesis since these nuclei present waiting points in the rapid-proton capture ($rp$) process [22,23] and such isomers may influence the proton-capture rates.

Low-lying $0^+$ states in medium-mass e-e nuclei have typical lifetimes in the order of a few ten to hundred ns [24] because the $E0$ decay proceeds entirely via IC and therefore is a relatively slow process [19]. However, the $2\gamma$ decay width varies strongly with the excitation energy, see Eq. (1), leading to extremely small branching ratios

($< 10^{-6}$) for $\omega_0 < 1$ MeV. Until now, searches for the $2\gamma$ emission from lower-energy $0^+$ states were unsuccessful, reporting only upper limits [25]. A $2\gamma$ decay at energies below 1 MeV was exclusively observed from the $11/2^-$ isomer in $^{137}$Ba using the fast-timing method [26,27]. Here, the single-photon decay is strongly hindered due to its highly unfavorable multipolarity ($M4/E5$).

Alternatively, if all bound electrons are removed the IC is disabled [28] and therefore $0^+$ states can only decay by $2\gamma$ emission to the ground state or by particle emission ($\alpha$ or $\beta$ decay) in unstable nuclides.

In this Letter we report the first direct measurement of the $2\gamma$ decay of the first excited $0^+$ state in stored, fully ionized $^{72}Ge^{32+}$ nuclei. This isomer, with an excitation energy of 691.43(4) keV [29], possesses a half-life of 444.2(8) ns in neutral atoms [30]. However, when it is fully ionized, the partial half-life for this isolated decay can be estimated to extend to several hundred ms, using the average value of the previously determined $M_{\gamma\gamma}$ matrix elements [10,16]. By combining the isochronous mode of a storage ring with nondestructive single-ion-sensitive Schottky detectors, the new experimental technique termed combined Schottky plus isochronous mass spectrometry (S + IMS), we were able to resolve the isomeric state and measure the time evolution of the number of observed isomers with a resolution of the order of ms. The thereby developed method is a sensitive approach to search for unknown excited $0^+$ states in exotic nuclei and for the study of their $2\gamma$ decays.

The experiment was conducted at the Gesellschaft für Schwerionenforschung (GSI) accelerator facility, using a primary $^{78}$Kr beam that was accelerated to an energy of precisely 441 MeV/nucleon (see below) using the heavy-ion synchrotron SIS-18. After fast extraction the beam was impinged on a 10 mm thick $^9$Be production target placed in the transfer beamline towards the experimental storage ring (ESR). Few-nucleon removal reactions at relativistic energies are known to produce low-lying isomeric states with relatively high probability of up to 10%. The $^{72}$Ge fragments emerged from the target with a mean energy of 367.9 MeV/nucleon. At this relativistic energy the $^{72}$Ge ions were fully ionized and were transported and injected into the ESR. No additional beam purification was necessary, allowing the storage of a large number of fragments within the acceptance of the ESR.

The stored ions revolved in the ESR with frequencies of about 2 MHz. The revolution frequency ($f$), can be related to the mass-to-charge ($m/q$) ratio of the ions via the equation for storage ring mass spectrometry [31]:

$$\frac{\Delta f}{f} = -\frac{1}{\gamma_t^2}\frac{\Delta(m/q)}{m/q} + \frac{\Delta v}{v}\left(1 - \frac{\gamma^2}{\gamma_t^2}\right), \qquad (2)$$

where $v$ and $\gamma$ are the velocity and the Lorentz factor of the ions, respectively. The machine parameter $\gamma_t$ is related to the relative change of the orbit length, $C$, caused by a relative change of magnetic rigidity, $B\rho = mv\gamma/q$ [32]. Here, the ESR was set to $\gamma_t \approx 1.396$.

In order to measure short-lived states ($T_{1/2} < 1$ s), the ESR was tuned in the isochronous ion-optical mode, where the energy of the $^{72}$Ge ions was chosen to match the condition $\gamma \approx \gamma_t$. Hence, the term containing the velocity spread $\Delta v/v$ in Eq. (2) vanishes and the revolution frequency is a measure of the mass-to-charge ratio enabling isochronous mass spectrometry (IMS) [33]. Conventionally, the revolution frequencies in the IMS are measured by foil-based time-of-flight detectors [34,35], which, however, lead to a rapid loss of stored particles. To enable lifetime measurements of exotic short-lived nuclides, nondestructive highly sensitive cavity-based resonant Schottky detectors have been continuously developed at GSI in the course of the last decade [36–38]. These cavities react on the relativistic highly charged ions repeatedly passing through. The latest edition, resonant at 410 MHz [38], at about the 212th harmonic of the revolution frequency, has been employed here for the first time. Furthermore, a second, less-sensitive detector, resonant at 245 MHz [37] was also used. The power outputs from both detectors were amplified and fed into commercial real-time spectrum analyzers (RSA), which were set to digitize the power signal in a frequency span of ±20 kHz around the chosen central frequency with a sampling rate of 50 kHz. The central frequency was set on the revolution frequency of $^{72g}Ge^{32+}$. The data were processed with the code *iqtools* [39] and the particle identification was realized with the code *rionid* [40].

Combining the isochronous mode of a storage ring with the single-ion-sensitive Schottky detectors has been realized in the past [41,42], but was never applied to short-lived isotopes. Two high-resolution settings were achieved by using scrapers to tailor the momentum distribution of the stored ions of interest and, finally, allowing us to resolve the doublet composed of the isomer $^{72m}Ge^{32+}$ and the ground state $^{72g}Ge^{32+}$ (see Fig. 1). The measurements on $^{72}$Ge were performed in two separate runs, denoted as $i = (1, 2)$, which differed slightly in the achieved resolving power. The collected data contained (1) 102 injections (∼30 min of data taking) and (2) 2459 injections (∼9 h of data taking).

Injections containing up to three $^{72m}$Ge particles have been recorded. Individual decay times can be determined analogously to the single-particle decay spectroscopy method utilized in studies of electron capture decays in the ESR [43–45]. Alternatively, the spectra of individual injections can be summed up. The integrated noise power of every peak in the summed spectrum is then directly proportional to the corresponding number of stored particles. The validity of this analysis approach has been thoroughly tested by dedicated simulations and cross-checked by extracting individual decay times, the details of which will be published elsewhere.

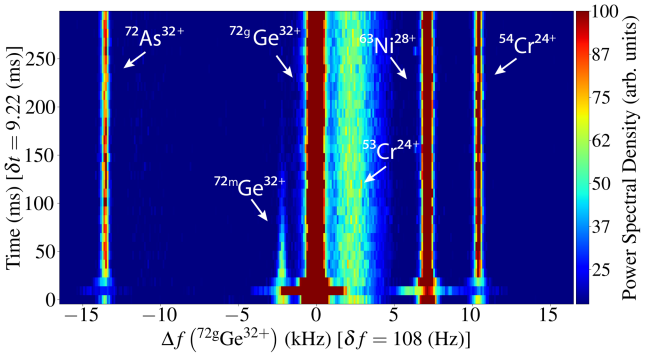


FIG. 1. Time after injection ($\delta t = 9.22$ ms per time bin) versus revolution frequency ($\delta f = 108$ Hz per frequency bin) spectrogram of the sum of 102 single injections (setting 1) centered on $^{72g}Ge^{32+}$ from 0 to 300 ms. The power spectral density of each ion species is proportional to their ion number.

To determine the partial half-life of the isomer, all spectra measured by both RSAs were adjusted in frequency by setting the center of the $^{72g}$Ge peaks to 0 Hz. Afterwards, the spectra were summed up separately for each RSA and data set. The resultant combined spectra of the 410 MHz detector during setting 1 is shown in Fig. 1. The traces corresponding to $^{72}As^{32+}$, $^{72m}Ge^{32+}$, $^{72g}Ge^{32+}$, $^{53}Cr^{24+}$, $^{63}Ni^{28+}$, and $^{54}Cr^{24+}$ are indicated. The slight distortion at the beginning of the measurement is due to kicker chamber eddy currents caused by switching off the injection magnets. Since it is the same for the traces of all stored ion species, it can be corrected for, except for the second time bin in which the shift is too fast to resolve it. We note that the observation of this distortion became possible thanks to the high temporal resolution of the new technique.

The decrease in intensity of the $^{72m}$Ge trace with time is evident. The peak areas for each time bin were extracted and fitted with an exponential function, see the inset in Fig. 2. The intensities of the stable species remained constant, thus indicating no considerable ion losses during the measurement period. The 245 MHz detector has a smaller quality factor than the 410 MHz one, which translates into a poorer signal-to-noise ratio and enlargement of scatter earlier in time due to background fluctuations. The derived lifetimes are tabulated in Table I. All values agree within the uncertainties. The average measured half-life for the $2\gamma$ in the rest frame is $T_{1/2}^{\text{rest}} = 23.9(6)$ ms determined by using the Lorentz factors of the $^{72m}$Ge ions in the isomeric states for each setting, $\gamma_1 = 1.3957(1)$ and $\gamma_2 = 1.3954(1)$.

From the parameters of the exponential fits, we can compute the initial number of isomers at $t = 0$ s. Together with the number of ions in the (stable) ground state we obtain an isomeric ratio of 3.4(2)%.

The measured frequencies and precisely known mass of $^{72}Ge^{32+}$ [46], allowed us to independently determine the excitation energy of the isomeric state. Data from both RSAs and for both settings (1,2) were analyzed separately.

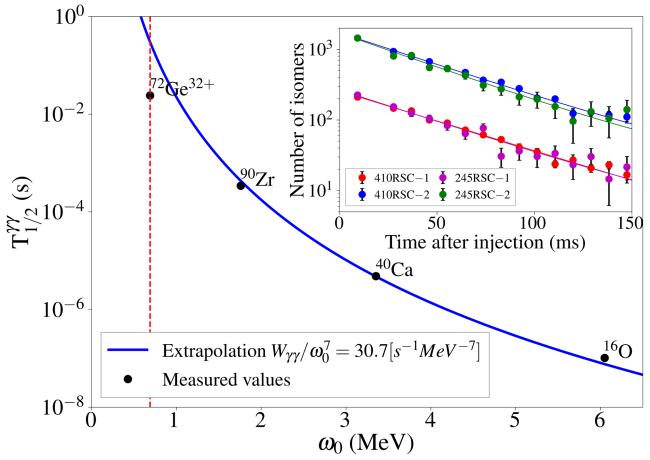


FIG. 2. Measured nuclear two-photon decay half-lives, taken from [10,16] and the present work, as a function of their excitation energy. The solid line corresponds to the curve obtained by considering the ratio of $W_{\gamma\gamma}$ and $\omega_0^7$ constant, with the constant being the average value of the sum of squares of the nuclear polarizabilities in Eq. (1). The vertical red dotted line is placed at the excitation energy of the isomeric state of $^{72}$Ge. The inset figure shows the evolution of the number of isomers in time for each setting in each detector used.

All obtained $\omega_0$ values, see Table II, are in good agreement with the tabulated excitation energy [29].

In Fig. 2 our new result for the $2\gamma$ decay in $^{72}$Ge is plotted together with the previous data on other nuclei for $0^+ \rightarrow 0^+$ $2\gamma$ transitions. The solid line is an extrapolation of these previously obtained results for higher excitation energies and thus shorter half-lives to the low-energy region using the scaling suggested by Eq. (1). For the case of the first excited state in $^{72}$Ge, the measured partial half-life is approximately 10 times shorter than suggested by the scaling law. This implies that the sum of all contributions in Eq. (1) ($M_{\gamma\gamma} = 70(2) \times 10^{-3}$ fm$^3$) is larger than the ones obtained in previous experiments. However, without measuring the angular correlation of the $\gamma$ rays, as could be done in Refs. [10,16], it is not possible to determine $\alpha_{E1}^2$ and $\chi_{M1}^2$ individually. We therefore have to rely on shell-model calculations to estimate the $M1$ contribution.

TABLE I. Measured lifetimes in the laboratory frame and half-lives in the rest frame for the different data subsets ($i$) in each Schottky detector. The last column corresponds to the weighted average of the values obtained with each detector. The insert of Fig. 2 shows the experimental data from which the decay constants have been obtained.

| Detector | $i$ | $\tau^{\text{lab}}$/ms | $T_{1/2}^{\text{rest}}$/ms | $\bar{T}_{1/2}^{\text{rest}}$/ms |
|---|---|---|---|---|
| $SD_{410}$ | 1 | 51.0(35) | 25.4(17) | 23.9(6) |
| | 2 | 47.7(13) | 23.7(6) | |
| $SD_{245}$ | 1 | 48.1(41) | 23.9(20) | 22.7(11) |
| | 2 | 44.5(28) | 22.1(14) | |

TABLE II. Measured frequency difference $\Delta f$ between the isomeric and ground state and the deduced excitation energy $\omega_0$ of the isomer for the two different data subsets ($i$) in each Schottky detector. The last column corresponds to the weighted average of the values obtained with each detector.

| Detector | $i$ | $\Delta f$/Hz | $\omega_0$/keV | $\overline{\omega_0}$/keV |
|---|---|---|---|---|
| $SD_{410}$ | 1 | 2162(8) | 694.4(31) | 692.8(19) |
| | 2 | 2157(4) | 691.8(24) | |
| $SD_{245}$ | 1 | 1301(7) | 699.7(43) | 695.0(32) |
| | 2 | 1290(4) | 692.8(29) | |

The transitional magnetic-dipole susceptibility consists of a paramagnetic and a diamagnetic term [8–10]:

$$\chi_{M1}^2 = \chi_p^2 + \chi_d^2 + 2\chi_p\chi_d \tag{3}$$

$$\chi_p = -\frac{8\pi}{9}\sum_n \frac{\langle 0_1^+\|M(M1)\|1_n^+\rangle\langle 1_n^+\|M(M1)\|0_2^+\rangle}{E(1_n^+) - E(0_1^+) - \frac{1}{2}[E(0_2^+) - E(0_1^+)]}, \tag{4}$$

$$\chi_d = -\frac{e^2}{6m}\langle 0_1^+\|r^2\|0_2^+\rangle. \tag{5}$$

Shell-model calculations using the $jj44$ model space and the JUN45 Hamiltonian [47], and an effective $M1$ operator [47], were performed to determine the paramagnetic contribution. In neighboring $^{74}$Ge the measured $M1$ strength distribution up to 5 MeV is in good agreement with these calculations [48]. Adding up the contributions from all theoretically expected $1^+$ states up to an excitation energy of 7.5 MeV results in a contribution from the magnetic-dipole transition susceptibility of $|\chi_p| \approx 3.2 \times 10^{-3}$ fm$^3$. There is a strong cancellation in the terms in Eq. (4) as a function of $E_i$; if one adds just the magnitudes, the result is about four times larger. The $jj44$ model space does not include $M1$ strength coming from the $0f_{7/2}$ to $0f_{5/2}$ contribution. The diamagnetic contribution can be estimated from the known $E0$ matrix element [19] as $|\chi_d| \approx 0.58 \times 10^{-3}$ fm$^3$. Therefore, the total transitional magnetic-dipole susceptibility is $|\chi_{M1}| \approx 3.8 \times 10^{-3}$ fm$^3$, which is small compared to the measured value of $M_{\gamma\gamma}$ and not too different to the values obtained in Ref. [10] in doubly magic nuclei.

The electric transition polarizabilities for $0_2^+ \to 0_1^+$ transitions are defined by Eq. (A.24) in [10] as

$$\alpha_{EL} = \frac{8\pi}{(2L+1)^2}\sum_n \frac{\langle 0_1^+\|i^L M(EL)\|I_n\rangle\langle I_n\|i^L M(EL)\|0_2^+\rangle}{E(I_n) - E(0_1^+) - \frac{1}{2}[E(0_2^+) - E(0_1^+)]}. \tag{6}$$

For the case of low-lying $0^+$ states, the electric-quadrupole transition polarizability $\alpha_{E2}$ may also become important. By using the reduced $E2$ matrix elements from both $0^+$ states to the two lowest-lying $2^+$ states of $^{72}$Ge [49], which usually exhaust more than 90% of the $E2$ strength, $\alpha_{E2}$ can be estimated via Eq. (6) to be $|\alpha_{E2}| \approx 4749$ fm$^5$. Therefore, the nuclear matrix element associated with $2E2$ transitions amounts to

$$M_{E2} = \sqrt{\omega_0^4 \frac{\alpha_{E2}^2}{4752}} \approx 0.8 \times 10^{-3} \text{ fm}^3. \tag{7}$$

Obtaining a theoretical estimate for the electric-dipole transition polarizability via shell-model calculations requires including contributions from orbital transitions related to the giant dipole resonance region that lie outside of the $jj44$ model space. Other theoretical approaches, such as the quasiparticle random-phase approximation, are also not applicable here since the two $0^+$ states in $^{72}$Ge are strongly mixed [49]. A more complete set of calculations for the $2\gamma$ matrix elements remains to be carried out. However, in view of the theoretically expected small contribution from the magnetic-dipole susceptibility and from the electric-quadrupole polarizability, it can be concluded that the electric-dipole transition polarizability is largely dominating the observed increase in transition strength. This finding is consistent with the presumed cancellation effect of the electric-dipole transition polarizability in the doubly magic nuclei, which should not be as pronounced in the midshell nucleus $^{72}$Ge.

In summary, we reported the results of the combined Schottky + isochronous mass spectrometry (S + IMS) applied to the direct determination of the excitation energy and partial half-life of an isomer in the millisecond regime with high precision. This represents a dramatic extension of the storage-ring based nondestructive lifetime spectroscopy to shorter-lived species as compared to previous experiments with electron-cooled stored beams [50]. A mass resolving power of $9.1 \times 10^5$ has been achieved, which allows us to fully resolve low-lying ($\sim$100 keV) isomers. For the $2\gamma$ decay of the $0^+$ isomer in $^{72}$Ge, a partial half-life of $T_{1/2}^{\text{rest}} = 23.9(6)$ ms and an excitation energy of $\omega_0 = 692.8(19)$ keV have been determined. The obtained partial half-life is a factor $\sim$10 shorter than expected from the extrapolation of previous results based on doubly magic $^{16}$O, $^{40}$Ca, and semi-magic $^{90}$Zr, indicating that the cancellation effect observed in those nuclides appears not to be present. This technique will be further developed and applied to the study of $^{98m}$Mo and $^{98m}$Zr.

Further experiments using direct $\gamma$-ray spectroscopy of the $2\gamma$ decay branch in $^{72}$Ge should elucidate the role of the magnetic and electric-dipole terms. In view of the shorter than expected lifetime, leading to a larger branching ratio for the $2\gamma$ decay channel in neutral atoms, such an experiment seems nowadays feasible utilizing high-efficiency gamma-ray spectrometers.

The authors thank the GSI accelerator team for providing excellent technical support. The results presented here are based on the experiment E143, which was performed at the

ESR at the GSI Helmholtzzentrum für Schwerionenforschung, Darmstadt (Germany) in the context of FAIR Phase-0. The authors also thank G. Hudson-Chang for proofreading. B. A. B. acknowledges the support from the NSF Grant No. PHY-2110365. P. K. acknowledges the support from BMBF under Grant No. NuSTAR.DA 05P19RDFN1. T. Y. was partly supported by JSPS KAKENHI Grant No. T23KK0055. I. D., C. G., and G. T. L. ackowledge funding by the Natural Sciences and Engineering Research Council of Canada (NSERC) (Grant No. SAPIN-2019-00030). Work at A. N. L. is supported by the U.S. Department of Energy, Office of Science, Office of Nuclear Physics, under Contract No. DE-AC02-06CH11357. This work was supported by the Slovenian Research and Innovation Agency under Grants No. I0-E005 and No. P1-0102, by the European Research Council (ERC) under the European Union's Horizon 2020 research and innovation programme (ERC-AdG NECTAR, Grant Agreement No. 884715; ERC-CoG ASTRUm, Grant Agreement No. 68284), the State of Hesse (Germany) within the Research Cluster ELEMENTS (Project ID 500/10.006), and by the STFC (UK).

*Deceased.
†D.FreireFernandez@gsi.de
‡W.Korten@cea.fr

[1] I. Tews, T. Krüger, K. Hebeler, and A. Schwenk, Neutron matter at next-to-next-to-next-to-leading order in chiral effective field theory, Phys. Rev. Lett. **110**, 032504 (2013).
[2] A. Tamii *et al.*, Complete electric dipole response and the neutron skin in $^{208}$Pb, Phys. Rev. Lett. **107**, 062502 (2011).
[3] B. Romeo, J. Menéndez, and C. Peña Garay, $\gamma\gamma$ decay as a probe of neutrinoless $\beta\beta$ decay nuclear matrix elements, Phys. Lett. B **827**, 136965 (2022).
[4] M. Göppert, Über die wahrscheinlichkeit des zusammenwirkens zweier lichtquanten in einem elementarakt, Naturwissenschaften **17**, 932 (1929).
[5] M. Göppert-Mayer, Über elementarakte mit zwei quantensprüngen, Ann. Phys. (Berlin) **401**, 273 (1931).
[6] D. Grechukhin, Two-quantum transitions of atomic nuclei (II), Nucl. Phys. **47**, 273 (1963).
[7] J. Eichler, Comment on two-photon emission of x rays, Phys. Rev. A **9**, 1762 (1974).
[8] J. Friar and M. Rosen, Dispersion corrections to elastic electron scattering by $^{12}$C and $^{16}$O II. On the use of the closure approximation, Ann. Phys. (N.Y.) **87**, 289 (1974).
[9] J. Friar, Low-energy theorems for nuclear Compton and Raman scattering and $0^+ \to 0^+$ two-photon decays in nuclei, Ann. Phys. (N.Y.) **95**, 170 (1975).
[10] J. Kramp *et al.*, Nuclear two-photon decay in $0^+ \to 0^+$ transitions, Nucl. Phys. **A474**, 412 (1987).
[11] S. Gorodetzky, G. Sutter, R. Armbruster, P. Chevallier, P. Mennrath, F. Scheibling, and J. Yoccoz, Double gamma emission in the 6.06-MeV monopole transition of $O^{16}$, Phys. Rev. Lett. **7**, 170 (1961).
[12] D. E. Alburger and P. D. Parker, Search for double gamma-ray emission from the first excited states of $O^{16}$ and $C^{12}$, Phys. Rev. **135**, B294 (1964).
[13] P. Harihar, J. D. Ullman, and C. S. Wu, Search for double gamma emission from the first excited states of $Ca^{40}$ and $Zr^{90}$, Phys. Rev. C **2**, 462 (1970).
[14] Y. Nakayama, Two-photon decay of the 1.76-MeV $0^+$ state of $^{90}$Zr, Phys. Rev. C **7**, 322 (1973).
[15] J. C. Vanderleeden and P. S. Jastram, Search for double-photon decay in $Zr^{90}$, Phys. Rev. C **1**, 1025 (1970).
[16] J. Schirmer, D. Habs, R. Kroth, N. Kwong, D. Schwalm, M. Zirnbauer, and C. Broude, Double gamma decay in $^{40}$Ca and $^{90}$Zr, Phys. Rev. Lett. **53**, 1897 (1984).
[17] J. N. Orce, C. Ngwetsheni, and B. A. Brown, Global trends of the electric dipole polarizability from shell-model calculations, Phys. Rev. C **108**, 044309 (2023).
[18] K. Heyde and J. L. Wood, Shape coexistence in atomic nuclei, Rev. Mod. Phys. **83**, 1467 (2011).
[19] T. Kibedi, A. Garnsworthy, and J. Wood, Electric monopole transitions in nuclei, Prog. Part. Nucl. Phys. **123**, 103930 (2022).
[20] A. N. Andreyev *et al.*, A triplet of differently shaped spin-zero states in the atomic nucleus $^{186}$Pb, Nature (London) **405**, 430 (2000).
[21] E. Bouchez *et al.*, New shape isomer in the self-conjugate nucleus $^{72}$Kr, Phys. Rev. Lett. **90**, 082502 (2003).
[22] H. Schatz *et al.*, rp-process nucleosynthesis at extreme temperature and density conditions, Phys. Rep. **294**, 167 (1998).
[23] Y. Sun, M. Wiescher, A. Aprahamian, and J. Fisker, Nuclear structure of the exotic mass region along the rp process path, Nucl. Phys. **A758**, 765 (2005).
[24] S. Garg, B. Maheshwari, B. Singh, Y. Sun, A. Goel, and A. K. Jain, Atlas of nuclear isomers—Second edition, At. Data Nucl. Data Tables **150**, 101546 (2023).
[25] J. Henderson *et al.*, Upper limit on the two-photon emission branch for the $0_2^+ \to 0_1^+$ transition in $^{98}$Mo, Phys. Rev. C **89**, 064307 (2014).
[26] C. Walz, H. Scheit, N. Pietralla, T. Aumann, R. Lefol, and V. Yu. Ponomarev, Observation of the competitive double-gamma nuclear decay, Nature (London) **526**, 406 (2015).
[27] P.-A. Söderström *et al.*, Electromagnetic character of the competitive $\gamma\gamma/\gamma$-decay from $^{137m}$Ba, Nat. Commun. **11**, 3242 (2020).
[28] Y. Litvinov *et al.*, Observation of a dramatic hindrance of the nuclear decay of isomeric states for fully ionized atoms, Phys. Lett. B **573**, 80 (2003).
[29] Brookhaven National Laboratory, Evaluated Nuclear Structure Data File, https://www.nndc.bnl.gov/ensdf/ (2020).
[30] G. Braun, A. Bockisch, and W. Neuwirth, Lifetime of the $0_2^+$ state of $^{72}$Ge determined by delayed auto-coincidence of a Ge(Li) detector, Nucl. Instrum. Methods Phys. Res. **224**, 112 (1984).
[31] B. Franzke, H. Geissel, and G. Münzenberg, Mass and lifetime measurements of exotic nuclei in storage rings, Mass Spectrom. Rev. **27**, 428 (2008).
[32] M. Steck and Y. A. Litvinov, Heavy-ion storage rings and their use in precision experiments with highly charged ions, Prog. Part. Nucl. Phys. **115**, 103811 (2020).

[33] M. Hausmann *et al.*, First isochronous mass spectrometry at the experimental storage ring esr, Nucl. Instrum. Methods Phys. Res., Sect. A **446**, 569 (2000).
[34] J. Trötscher *et al.*, Mass measurements of exotic nuclei at the ESR, Nucl. Instrum. Methods Phys. Res., Sect. B **70**, 455 (1992).
[35] B. Mei *et al.*, A high performance time-of-flight detector applied to isochronous mass measurement at CSRe, Nucl. Instrum. Methods Phys. Res., Sect. A **624**, 109 (2010).
[36] F. Nolden *et al.*, A fast and sensitive resonant schottky pick-up for heavy ion storage rings, Nucl. Instrum. Methods Phys. Res., Sect. A **659**, 69 (2011).
[37] M. S. Sanjari *et al.*, A resonant schottky pickup for the study of highly charged ions in storage rings, Phys. Scr. **2013**, 014088 (2013).
[38] M. S. Sanjari, D. Dmytriiev, Yu. A. Litvinov, O. Gumenyuk, R. Hess, R. Joseph, S. A. Litvinov, M. Steck, and Th. Stöhlker, A 410 MHz resonant cavity pickup for heavy ion storage rings, Rev. Sci. Instrum. **91**, 083303 (2020).
[39] M. S. Sanjari, iqtools: Collection of code for working with offline complex valued time series data in Python, Zenodo, 10.5281/ZENODO.761569 (2023).
[40] D. Freire-Fernández and G. Hudson-Chang, RionID: Collection of code for the identification of ringed ions in PYTHON, Zenodo, 10.5281/ZENODO.8169341 (2023).
[41] B. Sun *et al.*, A new resonator schottky pick-up for short-lived nuclear investigations, GSI Sci. Rep. **2010**, 163 (2011), https://repository.gsi.de/record/53521.
[42] X. L. Tu *et al.*, First application of combined isochronous and schottky mass spectrometry: Half-lives of fully ionized $^{49}Cr^{24+}$ and $^{53}Fe^{26+}$ atoms, Phys. Rev. C **97**, 014321 (2018).
[43] Y. Litvinov *et al.*, Observation of non-exponential orbital electron capture decays of hydrogen-like $^{140}Pr$ and $^{142}Pm$ ions, Phys. Lett. B **664**, 162 (2008).
[44] P. Kienle *et al.*, High-resolution measurement of the time-modulated orbital electron capture and of the $\beta+$ decay of hydrogen-like $^{142}Pm^{60+}$ ions, Phys. Lett. B **726**, 638 (2013).
[45] F. Ozturk *et al.*, New test of modulated electron capture decay of hydrogen-like $^{142}Pm$ ions: Precision measurement of purely exponential decay, Phys. Lett. B **797**, 134800 (2019).
[46] M. Wang, W. Huang, F. Kondev, G. Audi, and S. Naimi, The AME 2020 atomic mass evaluation (II). Tables, graphs and references, Chin. Phys. C **45**, 030003 (2021); The numerical table used was taken from the Atomic Mass Data Center: https://www-nds.iaea.org/amdc/.
[47] M. Honma, T. Otsuka, T. Mizusaki, and M. Hjorth-Jensen, New effective interaction for $f_5pg_9$-shell nuclei, Phys. Rev. C **80**, 064323 (2009).
[48] S. R. Johnson *et al.*, Testing shell-model interactions at high excitation energy and low spin: Nuclear resonance fluorescence in $^{74}Ge$, Phys. Rev. C **108**, 024315 (2023).
[49] A. Ayangeakaa *et al.*, Shape coexistence and the role of axial asymmetry in $^{72}Ge$, Phys. Lett. B **754**, 254 (2016).
[50] Y. A. Litvinov and F. Bosch, Beta decay of highly charged ions, Rep. Prog. Phys. **74**, 016301 (2011).